Damage Characterisation Of Thermally-Shocked Woven-Fibre-Reinforced Ceramic Matrix Composites

Christos Kastritseas, Paul A. Smith, Julie A. Yeomans

School of Engineering (H6), University of Surrey, Guildford, Surrey GU2 7XH, UK

ABSTRACT

Heated rectangular specimens of woven Nicalon^{TM}-fibre calcium aluminosilicate (CAS)-matrix composites were thermally-shocked by quenching into room-temperature water through a range of temperature differentials (ΔT=300-800˚C). Crack morphologies were assessed by reflected light microscopy (RLM) and scanning electron microscopy (SEM). The use of image assembling software allowed the generation of RLM images of all thermally-shocked surfaces onto which the crack patterns were then superimposed. This allowed clear identification of damage mechanisms and accurate quantification of damage accumulation with increasing thermal shock severity. Damage was first detected after quenching through ΔT=400˚C and consisted of matrix cracks of various orientations. These cracks were found to be mostly surface features but their morphology, as well as their density, was significantly affected by increasing shock severity. At the higher temperature differentials (ΔT=700-800˚C) fibre fractures could also be seen. The bi-axial nature of thermal shock-induced stresses and the degradation of the carbon-rich fibre/matrix interface were determined to be the factors that mainly influenced the onset and evolution of the observed cracking phenomena.

1. INTRODUCTION

As fibre-reinforced ceramic matrix composites (CMCs) are being considered increasingly for high-performance engines and other applications it is becoming apparent that there is a need to understand better their behaviour under conditions of 'thermal shock'. This term describes an event in which a sudden (usually downward) temperature change, or steady-state thermal gradient, generates stresses in the material that can lead to cracking and long-term property degradation [1]. Such events are common in high-temperature machinery, e.g. in the case of an emergency shut-down of a gas turbine. To date, only a limited number of papers have been published regarding the thermal shock behaviour of fibre-reinforced CMCs [2-6] while a consistent theoretical treatment of the problem does not exist. The present study builds upon previous work conducted at the University of Surrey on the thermal shock behaviour of glass ceramic-matrix CMCs containing unidirectional (UD) [5] and cross-ply [7] reinforcement architectures and the mechanical behaviour of woven fibre composites [8]. The main objectives were to determine the 'critical quenching temperature difference (or 'critical temperature drop'), ΔT_c, for the onset of damage due to thermal shock in CMCs with woven fibre reinforcement, to identify and differentiate between different damage mechanisms, and to monitor their development with increasing severity of thermal shock treatment, i.e. for increasing applied ΔTs.

2. MATERIAL AND EXPERIMENTAL TECHNIQUES

2.1. Material

The material comprised a calcium aluminosilicate (CAS) glass ceramic-matrix reinforced with cloths of woven (plain weave) silicon carbide fibres, which had been manufactured by hot pressing 12 plies of woven Nicalon^{TM}-fibre cloth impregnated with the matrix material to give a plate 215 x 75 (mm), with a thickness of 2.1 mm and low porosity. The fibre volume fraction was 0.35. Samples with dimensions 12 x 6 x 2.2 (mm) were cut from the supplied material and material surfaces for subsequent damage observation were polished to a 1μm surface finish. An as-polished surface can be seen in Fig.1, which shows the high quality of the surface finish obtained.

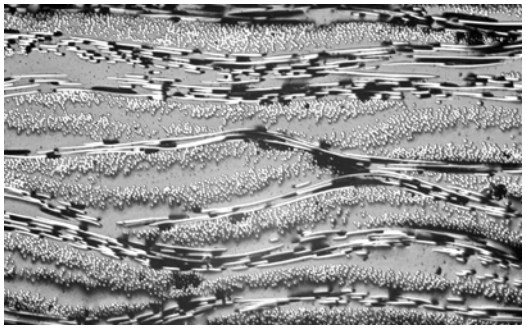

Fig.1. Reflected light micrograph of a polished as-received specimen surface

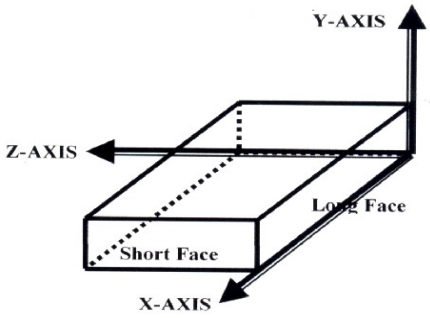

Fig.2. Nomenclature used to define the faces of test specimens

2.2. Thermal Shock Testing Procedure

The 'water-quench test' [1] was employed to produce the thermal shock condition. Each test specimen, after being heated for a short period of time in an electric muffle furnace at a pre-determined temperature, was rapidly dropped into a container with a large quantity (>10 l) of room-temperature (~20˚C) water. It was then removed from the water bath and allowed to dry before microscopic examination. The quenching temperature difference, ΔT, is defined as the difference between the temperature at which the material is held in the furnace and the temperature of the quenching medium. The critical quenching temperature difference, ΔT_c, is the temperature differential that results in the onset of material cracking. Temperature differentials between ΔT=300-800˚C were investigated, in increments of 100˚C. All specimens were initially held at high temperature for 15-20 minutes before quenching. It was found, however, that at the highest ΔTs investigated (ΔT=700-800˚C) this resulted in the formation of a thin glassy layer over the material surfaces, probably a by-product of oxidation processes, which obscured crack observation. To overcome this problem, specimens were held at the highest temperatures for shorter periods of time, i.e. 7-10 minutes.

2.3. Damage Observation and Quantification

Microscopic examination of the thermally-shocked specimens was carried out mainly using reflected light microscopy. Each surface under investigation was photographed section by section and the stored images were then assembled using suitable image assembling software to produce an image of the whole surface. The cracking pattern was imposed manually on the resulting image after careful observation of the real surface using microscopy. More detailed observation of crack patterns was also performed using a scanning electron microscope. The shock-induced damage was quantified in terms of the number of cracks per unit area and the crack length per unit area.

2.4. Nomenclature

The nomenclature used to describe damage is given in Fig. 2. The two surfaces of the specimen under investigation were the longitudinal (x-y) plane and the transverse (y-z) plane, which are designated as the 'long face' and the 'short face' respectively. From the specimen dimensions supplied in § 2.1 it can be seen that long faces were twice the size of short ones. Close observation of typical images, e.g. Fig. 1, reveals that both long and short faces of the woven material can be viewed as containing three types of areas: those that contain undulating longitudinal fibres, those containing transverse fibres (i.e. pointing into the surface), and areas of 'pure' matrix material (i.e. without reinforcement). If the first are termed '0˚ plies', the second '90˚ plies', and the third 'pure matrix plies', the woven material can be idealised, for damage description purposes, as a laminate containing alternating 0˚, 90˚, and pure matrix plies.

3. RESULTS

3.1. The Critical Quenching Temperature Difference

No damage was observed on the surfaces of the specimens after quenching through temperature differentials lower than 400˚C. After quenching through ΔT=400˚C, matrix damage could be seen, using the optical microscope, in the form of very shallow, fine cracks. Thus, it was determined that the critical quenching temperature difference for the woven (plain weave) Nicalon-fibre CAS-matrix system is ΔT_c=400˚C.

3.2. Thermal Shock Damage Mechanisms

3.2.1. Overview

Two types of damage were identified on the surfaces of specimens thermally shocked through ΔT≥400˚C, namely 'Matrix Cracks' and 'Fibre Failures'. Matrix cracks can be further divided into two sub-groups by taking into account the orientation of the cracks relative to the horizontal direction (x-axis in long faces, z-axis in short faces): those that run perpendicular to the horizontal direction and those that run in parallel to the horizontal direction. Hence, cracking phenomena can be classified as:

a. Perpendicular Matrix Cracks
b. Horizontal Matrix Cracks
c. Fibre Failures

These damage modes were seen on both long and short faces of thermally-treated specimens.

3.2.2. Perpendicular Matrix Cracks

Perpendicular matrix cracks were the first form of thermal shock damage easily identifiable after quenching through ΔT≥400˚C. They were shallow surface features that ran mainly through pure matrix plies at right angles to the horizontal, and arrested when they encountered fibres in adjacent plies (Fig. 3). At higher ΔTs (ΔT≥600˚C), they could be seen to extend into adjacent 0˚ or 90˚ plies (Fig. 4).

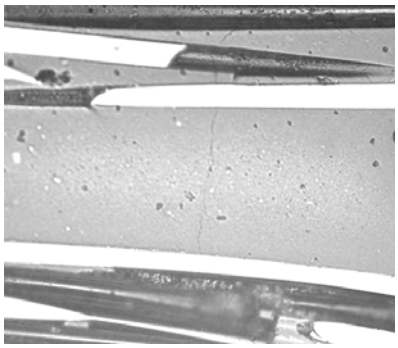

Fig.3. Perpendicular matrix crack in pure matrix ply at ΔT=400˚C

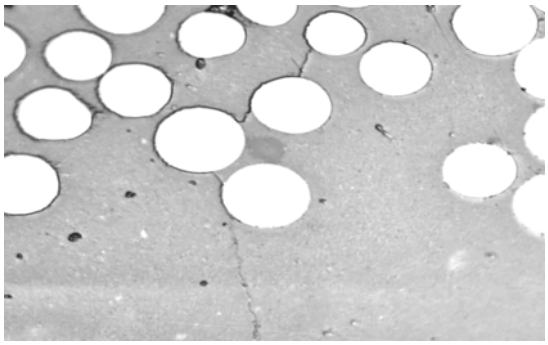

Fig.4. Perpendicular matrix crack extending in a 90˚ ply at ΔT=600˚C (fibre diameter is 15 μm)

A similar form of damage was detected in individual 0˚ plies, also at ΔT≥400˚C. These cracks were short in length, and spanned the matrix between two or three adjacent fibres (Fig. 5). However, observation and quantification of perpendicular cracks in 0˚ plies could not be taken any further due to the small width of these plies and the significant amount of unavoidable damage incurred to them during the specimen preparation stages.

3.2.3. Horizontal Matrix Cracks

Horizontal matrix cracks were observed uniquely in 90˚ plies (Fig. 6). The majority of these cracks were contained within the 90˚ plies with a small number arresting when they encountered adjacent plies. The critical quenching temperature difference for the onset of this damage mode could not be determined readily as cracks first appeared at ΔT=400˚C but were very short in length and originated from either the edges of the specimen or pre-existing

damage (e.g. voids) in the 90˚ plies. Fully formed cracks that did not originate from edges or pre-existing damage were visible only after quenching through ΔT=450˚C. Consequently, the critical quenching temperature differential for the onset of horizontal matrix cracking in the woven Nicalon/CAS is taken to be in the range of ΔT_c=400-450˚C.

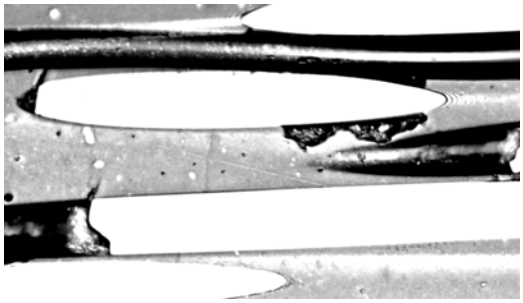

Fig.5. Perpendicular matrix crack inside a 0˚ ply.

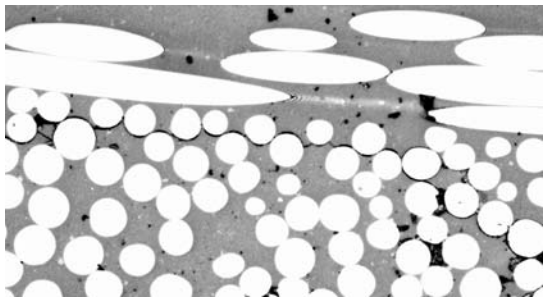

Fig.6. Horizontal matrix crack at ΔT=500˚C inside a 90˚ ply.

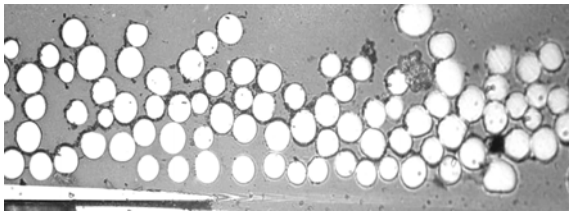

Fig.7. Horizontal matrix crack at ΔT=700˚C. The increase in length, depth and opening is evident.

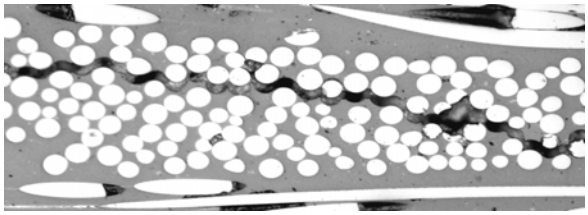

Fig.8. Horizontal matrix crack at ΔT=800˚C on a specimen held for 7-10 mins at high Temperature.

At higher temperature differentials, horizontal matrix cracks were observed to extend along the whole length of 90˚ plies or even penetrate into adjacent plies. In addition, their depth and opening increased significantly (Fig. 6-8).

3.2.4. Fibre Failures

Fibre failures occur when a perpendicular matrix crack does not arrest, change direction or circumvent a fibre in its path but runs through and breaks it. This phenomenon was observed at high temperature differentials (ΔT=700-800˚C) and can be associated with changes in the chemistry of the carbonaceous fibre-matrix interfaces that cause embrittlement of the material. The extent of such cracking was closely related to the time the specimen was held at high temperature, which dictated the extent of material degradation due to oxidation processes. Specimens held for 7-10 minutes at high temperature were found to contain few fibre failures (1-2 for ΔT=700˚C, 4-5 for ΔT=800˚C), whereas in specimens heated for 15-20 minutes fibre failures increased significantly, although no reliable quantification was possible as parts or the surfaces or whole surfaces were covered by a thin glassy film. Fibre failures at ΔT=700˚C on specimens heated for 7-10 minutes and 15-20 minutes can be seen in Figs. 9 and 10 respectively. It should also be noted that some microstructural degradation was evident even at ΔT=600˚C. However, no fibre failures were detected at this temperature differential.

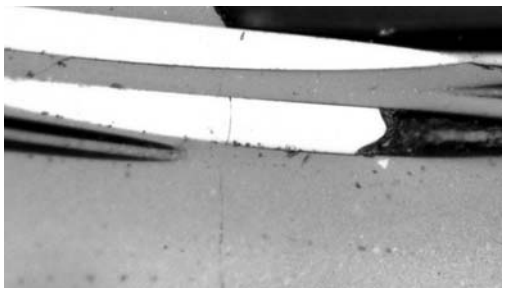

Fig. 9. Fibre failure at ΔT=700˚C on specimen heated for 7-10 mins

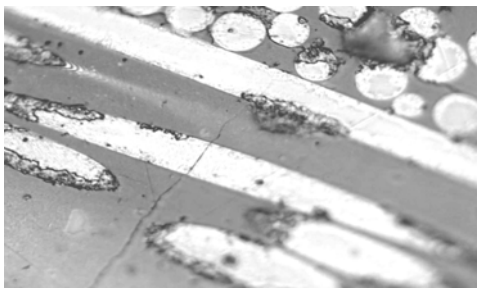

Fig.10. Fibre failure at ΔT=700˚C on specimen heated for 15-20 mins

3.3. Quantification of Thermal Shock Damage

Changes in the respective densities of perpendicular and horizontal matrix cracks with increasing severity of thermal shock are described in this section for both long and short faces. Crack densities quantified as cracks per unit area are presented in Fig. 11, while crack densities in terms of crack length per unit area are shown in Fig. 12.

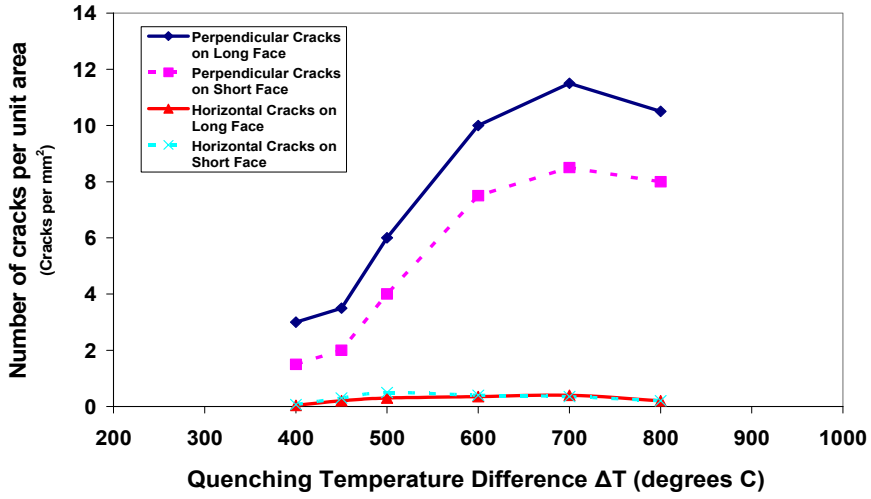

Fig. 11. Changes in perpendicular and horizontal matrix crack density as a function of increasing ΔT in terms of crack number per unit area on long and short faces

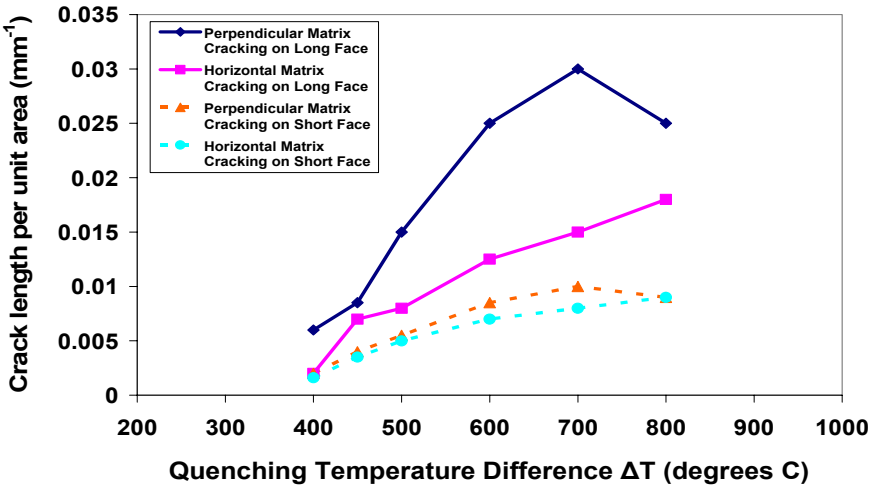

Fig. 12. Changes in perpendicular and horizontal matrix crack density as a function of increasing ΔT in terms of crack length per unit area on long and short faces

Clear trends emerge from both methods of quantifying perpendicular matrix cracks. The density of these cracks increases at an almost constant rate for ΔT=400-600˚C. The rate of increase can be seen to decrease for ΔT=600-700˚C and crack density reaches a maximum at ΔT=700˚C. A decrease in its value can be observed for ΔT=700-800˚C, and at ΔT=800˚C it is comparable to that at ΔT=600˚C. The density of horizontal matrix cracks shows a steady, continuous increase with increasing ΔT (see Fig.12) and reaches a maximum at ΔT=800˚C. However, Fig. 11 shows a minimal change in the number of cracks per unit area with increasing shock severity. This suggests that higher shocks mostly affect the morphology of horizontal matrix cracks, i.e. their length, depth, and opening.

It can also be noticed that both horizontal and perpendicular crack densities on long faces are much higher than the respective densities on short faces. This is confirmed by the images of Figs. 13(a) and (b), where observed crack patterns at ΔT=600˚C have been superimposed on a short face and an area of equal dimensions at the centre of a long face of a thermally-shocked specimen. Crack density on the long face is obviously much higher.

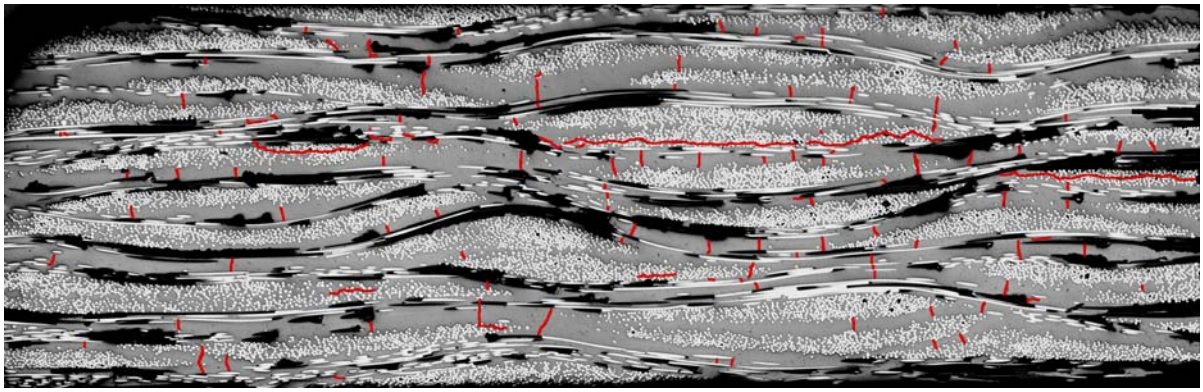

(a)

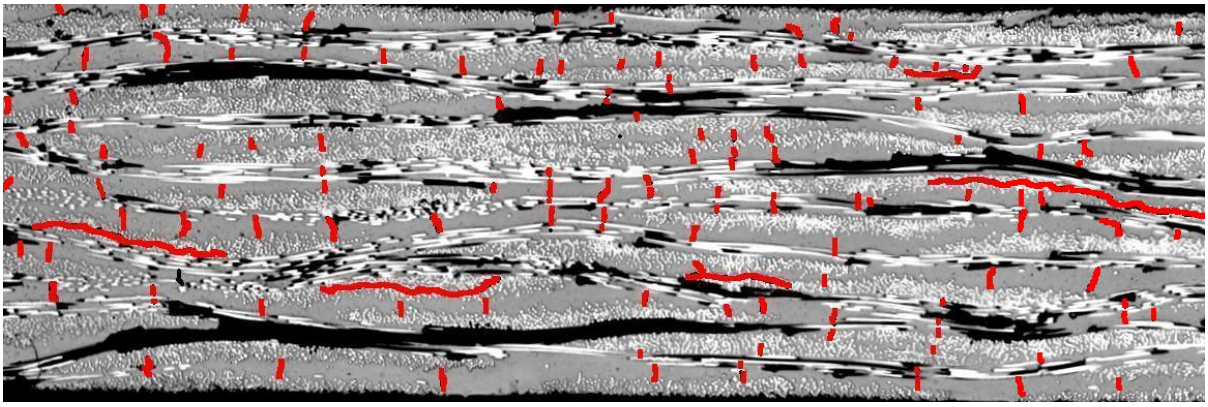

(b)

Fig. 13. Observed crack patterns at ΔT=600˚C superimposed on images of (a) a short face and (b) an area of equal dimensions at the centre of a long face of a thermally-shocked specimen.

4. DISCUSSION

The results reported in this paper are believed to be the first regarding thermal shock damage of a glass ceramic-matrix composite with woven fabric reinforcement. The main damage sustained by thermally-shocked specimens was in the form of matrix cracking. This is in agreement with published research on the thermal shock behaviour of fibre-reinforced CMCs [1-7] and was expected, since the matrix material is weaker than the fibres. At low and moderate ΔTs, advancing thermal shock-induced matrix cracks were deflected at the fibre/matrix interface leaving the fibres unaffected.

Observed damage modes were similar to the ones found in thermally-shocked UD and cross-ply Nicalon™/CAS, i.e. perpendicular cracks in regions of longitudinal fibres (0˚ plies) and horizontal cracks in regions containing transverse fibres (90˚ plies). Cracking in pure matrix plies was unique to this material as UD and cross-ply CMCs do not contain such regions. In addition, the presence of undulating fibres in the woven material did not affect crack initiation and development significantly. The critical temperature differentials for the onset of the observed damage modes were also similar to the ones reported for UD and cross-ply Nicalon™/CAS. An exception is the $(0^{\circ}/90^{\circ})_{3s}$ cross-ply Nicalon™/CAS, where horizontal cracking begins at $\Delta T=350^{\circ}C$. This implies that the stacking sequence may have an effect on the magnitude and distribution of the applied shock-induced thermal stress field.

This idea is reinforced if the orientation of each damage mode is considered more closely. As the applied stress field due to thermal shock is bi-axial in sense and dependent on material anisotropy, it can be concluded that the magnitudes of its components change from ply to ply depending on fibre presence and/or architecture. The magnitude of its horizontal component appears to be larger in 0˚ and pure matrix plies whereas the perpendicular component may dominate in 90˚ plies.

Damage modes due to thermal shock exhibited different behaviour for increasing ΔTs. Horizontal matrix cracks grew significantly in length and depth but their number did not change significantly. By contrast, perpendicular matrix cracks did not change in morphology (i.e. they remained surface features of small depth) but increased moderately in length and significantly in number. At high ΔTs they could be seen to be evenly distributed along the lengths of 0˚ and pure matrix plies, i.e. they attained almost constant crack spacings. This is similar to the situation under tensile testing [8], and implies that stress transfer takes place during thermal shock between fibre/matrix and between different plies. However, there are two major differences; first, crack densities under thermal shock were found to be at least an order of magnitude smaller than the ones measured under tensile testing [8]. In addition, whereas a definite ‘saturation’ point exists for damage accumulation under tensile testing, i.e. when crack density attains a maximum constant value not affected by increasing applied stress, this is not the case here. Instead, there is a ΔT for which a maximum crack density is measured, but application of higher thermal loads reveals reductions in crack density. Similar trends have also been reported for UD Nicalon/CAS [5].

Two conclusions can be drawn from the above observations. First, the stress transfer mechanism results in the energy available for cracking in pure matrix and 0˚ plies to be consumed mainly in multiplying the number of cracks; by contrast, in 90˚ plies, as no transfer takes place along the perpendicular direction, the energy available results in the extension (in length and depth) of a small number of cracks that appear at preferential sites in some 90˚ plies. Second, stress transfer between fibre/matrix and between plies under thermal shock appears to be less efficient than under pure tension (since cracking strains should be the same in both cases). Although interface degradation takes place at high ΔTs, it cannot explain the small crack densities at low ΔTs and does not affect significantly stress transfer between plies. However, as the thermal shock-induced stress field is bi-axial, apart from the axial component that causes cracking in pure matrix and 0˚ plies there is also a perpendicular component that acts at right angles to fibre/matrix and ply to ply interfaces. Such a stress component is not present under tensile testing, where loading is purely axial. This component can be thought of as affecting both fibre/matrix and ply-to-ply stress transfer through shear and, thus, reducing the efficiency of stress transfer under thermal shock.

At high ΔTs (>600˚C), material degradation due to oxidation processes became evident even after short-term high-temperature exposure. Oxidation of the fibre/matrix interface resulted in the occurrence of fibre cracks at ΔT=700˚C and ΔT=800˚C and contributed to the reduction in the rate of increase in perpendicular matrix crack density between ΔT=600-700˚C. For ΔT=700-800˚C material degradation resulted in a decrease in measured crack density. However, as a reduction in crack density was evident at ΔT=800˚C even after very short high-temperature exposure (where the degradation was not so widespread), this trend should also be attributed to boiling phenomena in the quenching medium that take place at high ΔTs and affect the properties of the applied thermal stress field [1].

It should also be noted that the onset of cracking, as well as the observed damage modes, were the same for both long and short faces. However, measured crack densities on long faces were much higher. This shows that while the severity of the shock was the same for both faces the energy available for cracking was larger in the long ones. This implies that an area effect exists that affects the extent of thermal shock-induced cracking, i.e. the larger the area the higher the energy available for cracking and consequently the higher the measured crack densities.

5. CONCLUDING REMARKS

Cracking phenomena due to thermal shock on the surfaces of water-quenched woven Nicalon™/CAS were described in detail in this paper. Damage modes were identified and their development for shocks of increased severity was documented. The characteristics of the observed damage phenomena were interpreted by considering the properties of the applied thermal stress field and the effect of high-temperature material degradation. Work is in hand to model these phenomena and to quantify their effect on the elastic properties of the material.

ACKNOWLEDGEMENTS

CK acknowledges financial support from the Engineering and Physical Sciences Research Council (UK) and the ‘Alexander S. Onassis’ Foundation.

References

1. **Wang, H.** and **Singh, R. N.**, “Thermal shock behaviour of ceramics and ceramic composites”, *Int. Mat. Rev.*, **39**/6 (1994), 228-244
2. **Kagawa, Y.**, **Kurosawa, N.** and **Kishi, T.**, “Thermal shock resistance of SiC fibre-reinforced borosilicate glass and lithium aluminosilicate matrix composites”, *J. Mater. Sci.*, **28** (1993), 735-741
3. **Wang, H.**, **Singh, R. N.** and **Lowden R. A.**, “Thermal shock behaviour of two-dimensional woven fiber-reinforced ceramic composites”, *J. Am. Ceram. Soc.*, **79**/7 (1996), 1783-1792
4. **Webb, J. A.**, **Singh, R. N.** and **Lowden R. A.**, “Thermal shock damage in a two-dimensional woven-fiber-reinforced-CVI SiC-matrix composite”, *J. Am. Ceram. Soc.*, **79**/11 (1997), 2857-2864
5. **Blissett, M. J.**, **Smith, P. A.** and **Yeomans, J. A.**, “Thermal shock behaviour of unidirectional silicon carbide fibre reinforced calcium aluminosilicate”, *J. Mater. Sci.*, **32** (1997), 317-325
6. **Boccaccini, A. R.**, **Janczak-Rusch, J.**, **Pearce, D. H.** and **Kern, H.**, “Assessment of damage induced by thermal shock in SiC-fibre-reinforced borosilicate glass composites”, *Comp. Sci. Tech.*, **59** (1999), 105-112

7. **Blissett, M. J.**, **Smith, P. A.** and **Yeomans, J. A.**, "Flexural mechanical properties of thermally treated unidirectional and cross-ply Nicalon-reinforced calcium aluminosilicate composites", *J. Mater. Sci.*, **33** (1998) 4181-4190
8. **Ironside, K. I.**, "Damage in Woven Ceramic Matrix Composites", Ph.D. Thesis, University of Surrey, 1996